AAPS PharmSciTech 2004; 5 (4) Article 58 (http://www.aapspharmscitech.org).

Heat and Mass Transfer Scale-up Issues during Freeze Drying: II. Control and Characterization of the Degree of Supercooling

Submitted: January 5, 2004; Accepted: August 5, 2004.

Shailaja Rambhatla,[1, 2] Roee Ramot,[1, 3] Chandan Bhugra,[1] and Michael J. Pikal[1]

[1]School of Pharmacy, University of Connecticut, Storrs, CT 06269

[2]Present address: Bayer HealthCare, Biological Products, Clayton, NC 27520

[3]Present address: School of Engineering, University of Connecticut, Storrs, CT 06269

Abstract

This study aims to investigate the effect of the ice nucleation temperature on the primary drying process using an ice fog technique for temperature-controlled nucleation. In order to facilitate scale up of the freeze-drying process, this research seeks to find a correlation of the product resistance and the degree of supercooling with the specific surface area of the product. Freeze-drying experiments were performed using 5% wt/vol solutions of sucrose, dextran, hydroxyethyl starch (HES), and mannitol. Temperature-controlled nucleation was achieved using the ice fog technique where cold nitrogen gas was introduced into the chamber to form an "ice fog," thereby facilitating nucleation of samples at the temperature of interest. Manometric temperature measurement (MTM) was used during primary drying to evaluate the product resistance as a function of cake thickness. Specific surface areas (SSA) of the freeze-dried cakes were determined. The ice fog technique was refined to successfully control the ice nucleation temperature of solutions within 1°C. A significant increase in product resistance was produced by a decrease in nucleation temperature. The SSA was found to increase with decreasing nucleation temperature, and the product resistance increased with increasing SSA. The ice fog technique can be refined into a viable method for nucleation temperature control. The SSA of the product correlates well with the degree of supercooling and with the resistance of the product to mass transfer (ie, flow of water vapor through the dry layer). Using this correlation and SSA measurements, one could predict scale-up drying differences and accordingly alter the freeze-drying process so as to bring about equivalence of product temperature history during lyophilization.

Keywords: nucleation, freeze-drying, scale-up, mass transfer.

Corresponding Author: Michael J. Pikal, School of Pharmacy, University of Connecticut, Storrs, CT 06269. Tel: 860-486-3202. Fax: 860-486-4998. Email pikal@uconnvm.uconn.edu.

Introduction

The first step of the lyophilization process involves freezing of a solution, which results in conversion of most of the water into ice, leaving the solute in a glassy and/or crystalline phase. This step is followed by primary drying, which involves the sublimation of ice. Secondary drying, or desorption, is the next stage where removal of unfrozen water occurs.

An important objective of the freezing step is to produce a homogeneous batch, which is challenging because of the random nature of nucleation. The ice nucleation temperature, Tn, is quite variable even in a well-controlled process. Intervial variation in nucleation temperatures causes heterogeneity in drying behavior, which can pose significant process control problems in the primary drying stage. The degree of supercooling, defined as the difference between the equilibrium freezing point and the temperature at which ice crystals first form in the sample, reflects random nucleation and also depends on the solution properties and process conditions.[1] The degree of supercooling governs the rate of nucleation and thus determines the number of ice crystals formed, which, in turn, affects the porosity of the freeze-dried cake.[2] A greater number of ice crystals results in a smaller pore size in the dried cake and hence a longer primary drying time.[2-5] The reduction in drying rate with increasing degree of supercooling is significant. A recent study[4] showed about a 3% increase in drying time for a 1°C decrease in ice nucleation temperature. Another study[6] found a 1% increase in primary drying time for 1°C decrease in nucleation temperature. Thus the impact of the degree of supercooling on drying behavior is both significant and variable.

The primary drying stage accounts for the greatest portion of the freeze-drying cycle, so optimization of primary drying is important. The rate of water removal during primary drying may be expressed as

$$\frac{dm}{dt} = \frac{A_p(P_0\text{-}P_c)}{\hat{R}_{ps}} \qquad (1)$$

where dm/dt is the rate of mass transfer for the water vapor, P_0 is the equilibrium vapor pressure of ice at the temperature of the frozen material, P_c is the chamber pressure, $\hat{R}_{ps}$ is the area normalized resistance of the dried product and stopper. Equation 1 assumes the usual conditions in primary

drying where essentially all gas in the chamber is water vapor. In nearly all cases, product resistance is much greater than the stopper resistance. Thus, the rate of water vapor removal depends on the product resistance, which, in turn, is a reflection of how the initial solution was frozen. That is, since it is the sublimation of ice that creates the pores in the solute matrix, the dimensions of the pores are a direct reflection of the size and geometry of the ice crystals formed during freezing.

The remaining unfrozen water, usually 15% to 20% wt/wt of solute, requires a secondary drying step, or a desorption step, for its removal, and is performed under vacuum at shelf temperatures that are higher than primary drying shelf temperatures. While a small "pore" size means greater resistance to flow of water vapor during primary drying, it also means greater surface area and hence faster desorption during secondary drying. Thus, freezing variations impact both primary and secondary drying.

Most laboratory freeze-drying processes occur on a shorter time scale than in a pharmaceutical production plant (ie, loading is faster) and in an environment that contains far more airborne "ice-nucleating" particles than a typical Class 100 production environment, thereby allowing ice nucleation at higher temperatures in the laboratory. Thus, a freezing procedure optimized in the laboratory may not transfer exactly to a manufacturing scale. The biggest effect probably arises from the cleaner air in the production environment, meaning fewer heterogeneous nucleation sites in the production solution and, hence, higher degrees of supercooling. Higher degrees of super-cooling means higher product resistance, and the freeze-drying cycle developed in the laboratory will produce slightly higher product temperature (≈1°C or more) and a longer primary drying process (≈10% or more) in manufacturing.[6] The extension in primary drying time is usually the more serious problem, particularly if unrecognized and fixed time cycles are used. It is thus important to be able to control the nucleation temperature in order to control product resistance and drying times.

Annealing the samples during the freezing step at temperatures well above the Tg′ of the formulation has been applied as one way to increase the primary drying rate and overcome the effect of heterogeneity in nucleation rates.[3] Ostwald ripening, a phenomenon that occurs during annealing, results in the formation of larger crystals (which means larger pores) at the expense of smaller ones, and is believed to be responsible for the significant increases in the primary drying rate observed upon annealing. In addition, variations in pore structure and drying behavior originating from variations in degree of supercooling can be largely removed by the annealing process. If annealing is not desirable for other reasons, such as the potential for phase separation, interfacial degradation, etc, the ability to control the nucleation temperature is of paramount importance in ensuring homogeneity in terms of pore size and drying times.

This research uses an ice fog technique for temperature-controlled nucleation. This concept was suggested by T. W. Rowe[7] in 1990 and involves purging cold nitrogen gas into the high humidity environment in the drying chamber to form an ice fog after the vials have achieved the temperature at which nucleation is desired. The details of the ice fog technique employed in this study and its application in temperature-controlled nucleation will be presented. Also, we explore the concept that specific surface area data for laboratory and clinical trials (ie, sterile) batches can be used to address scale-up issues.

The objective of this research is 2-fold: (1) to further develop the ice fog technique for controlling the nucleation temperature and producing samples freeze dried at selected nucleation temperatures; and (2) to establish a correlation between specific surface area (obtained from Brunauer-Emmett-Teller **[**BET]- specific surface area analysis) and product resistance (obtained from manometric temperature measurement [MTM]) for commonly used pharmaceutical excipients, in an effort to predict scale-up differences and accordingly modify the laboratory-designed freeze-drying process such that equivalent product temperature histories are obtained in manufacturing and development.

Materials and Methods

Materials

Crystalline sucrose, hydroxyethyl starch (HES), and dextran (molecular weight 41 kd) were obtained from Sigma Aldrich Co (St Louis, MO). D-mannitol USP was obtained from Ferro Pfansteihl Labs Inc (Waukegan, IL).

Vials used for freeze drying were 20-mL tubing vials from West Pharmaceutical Co (Lionville, PA). Stoppers were 20-mm finish gray butyl stoppers (West Pharmaceutical Co) designed for lyophilization.

Freeze Drying

Freeze drying was performed in a laboratory scale Durastop Freeze dryer (Kinetics Thermal Systems, Stone Ridge, NY) using 5% wt/vol solutions of the excipients mentioned previously. A thermal shield in the form of aluminum foil was used on the inside of the door to minimize heat transfer heterogeneity due to radiation heat transfer to edge vials.[8] Aqueous solutions of the solutes were prepared and filtered through a 0.45-µm membrane filter. In the case of HES, the solution was heated to 80°C for 30 minutes to facilitate dissolution and then cooled down to room temperature prior to filtration and vacuum degassing. Vials were filled with 5

mL of solution and loaded onto the temperature-controlled shelves of the freeze dryer. After the vials attained the temperature at which nucleation of samples was desired, the ice fog technique (as will be described later) was used to nucleate the samples at that temperature. Following nucleation, the shelf temperature was lowered to –40°C at 1°C/min to completely freeze the solution. Primary drying was conducted at shelf temperatures that enabled the product temperature to be below the collapse temperatures of the materials as determined from freeze drying microscopy studies. For mannitol, the shelf temperature was raised to +5°C during primary drying since the mannitol crystallized during freezing and may be freeze dried at higher temperature without collapse. MTM, as described later, was used to obtain pressure rise data at specific time intervals during primary drying, thereby allowing product resistance to be measured.[9] The end point of primary drying was determined from a sharp decrease in the dew point determined by an Ondyne moisture sensor (Endress+Hauser HydroGuard 2250, Greenwood, IN).[6] This electronic moisture sensor has the sensitivity to determine the presence of ice in less than 1% of the vials and, therefore, a sharp decrease in the dew point at the end of primary drying indicates that the composition of vapor in the drying chamber has shifted from nearly pure water to nearly pure nitrogen. Secondary drying was conducted at a shelf temperature of 40°C for 5 hours. Vials were stoppered and sealed under vacuum after secondary drying.

Temperature-Controlled Nucleation

The ice fog technique was used to nucleate samples at a selected temperature. The procedure involved lowering the shelf temperature and cooling the samples to the desired temperature of nucleation. Next, a flow of nitrogen gas was introduced into the chamber at a regulated pressure of 10 psig. The nitrogen gas at elevated pressure was circulated through copper coils immersed in liquid nitrogen before it entered the chamber. As cold nitrogen gas enters the humid chamber under pressure, ice crystals form and enter the vials due to the slight increase in pressure, resulting in the nucleation of the solution at the desired temperature. The temperature of the nitrogen gas at the entrance to the chamber was less than –40°C. Only 1 shelf containing ~100 vials was used for this study. Using the ice fog technique, nucleation was attempted at 3 different temperatures ranging from the highest temperature of –1°C (lowest degree of supercooling) to as low a temperature as possible (≈ –10°C, highest degree of supercooling). It was not possible to study higher degrees of supercooling in the laboratory because of the presence of particulate matter that caused nucleation even before the ice fog could be introduced.

Manometric Temperature Measurement

Product resistance during primary drying was obtained from manometric temperature measurement (MTM). In this technique, the valve connecting the chamber and the condenser is closed for 25 seconds and the chamber pressure is recorded every 0.25 seconds. The MTM equation is fit to the pressure rise data, P, obtained as a function of time, t, in order to obtain values of dried layer resistance as a function of cake thickness throughout primary drying.[9] The fit of the MTM equation to the data yields values of the vapor pressure of ice (P_i), from which the product temperature is determined, and the sum of the product and the stopper resistance, ($\hat{R}_{ps}$) is determined. An earlier study[10] evaluated the stopper resistance to be ~3% of the total resistance, which is small compared with the product resistance and, hence, the stopper resistance may be ignored. In this study, a constant value of 1.0°C was assumed for the temperature difference between the top and bottom of the frozen layer (ΔT_i).[9] An improved version of the MTM procedure evaluates ΔT_i from data.[9] In our calculations we found no difference in values of $\hat{R}_p$ and P_i calculated by the 2 procedures.

Specific Surface Area Measurements

A BET surface area analyzer, Flowsorb II (Micromeritics Instrument Corporation, Norcross, GA) was used to measure the specific surface area of the freeze-dried samples. Outgassing of samples was performed by heating the sample on a heating mantle at 35°C for 2 hours while flowing a mixture of helium and krypton gas through the sample. Calibration of the instrument was performed using 100% krypton gas at room temperature (≈22°C, or as recorded during the time of measurement) and at a pressure recorded during the time of measurement. A mixture of krypton and helium (0.1 mol% krypton in helium) was introduced into the sample with krypton being the adsorbate and helium the inert carrier gas. Single point measurements at 0.1 mol% krypton were performed. Reproducibility of specific surface areas was better than ±2%.

RESULTS AND DISCUSSION

Ice Fog Technique: Method 1

Freeze-drying experiments were performed using the ice fog technique as described in the experimental section to nucleate at 3 different temperatures (–3°C, –7°C, and –12°C). Ice nucleation temperatures were determined from product thermocouple data for 3 vials. Nucleation of contents of all vials required times ranging from nearly 10 minutes in one case to as long as 30 minutes in another. Primary drying of a 5% wt/vol sucrose solution was conducted at a shelf temperature

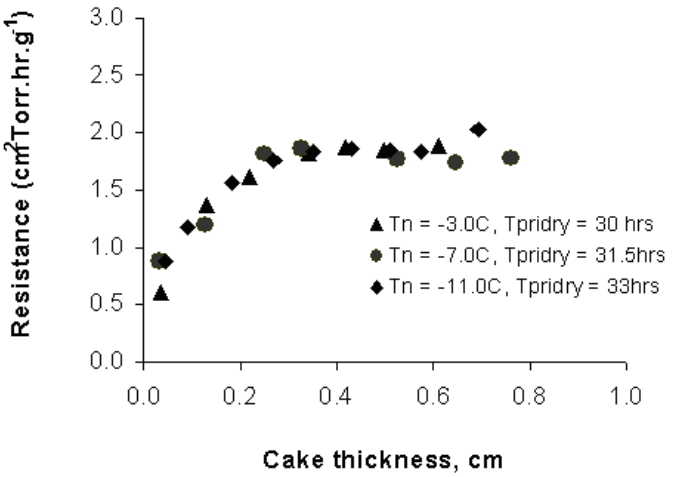

Figure 1. Resistance, $\hat{R}_{ps}$, ($\hat{R}_{ps} = \hat{R}_p + \hat{R}_s$) as a function of dry layer thickness obtained for 5% wt/vol sucrose using the ice fog method I at 3 different nucleation temperatures. $\langle \hat{R}_p \rangle$ values average resistance in cm^2 · Torr · hr · g^{-1} during primary drying are 1.76 (-3°C), 1.78 (-7°C), and 1.86 (-11°C).

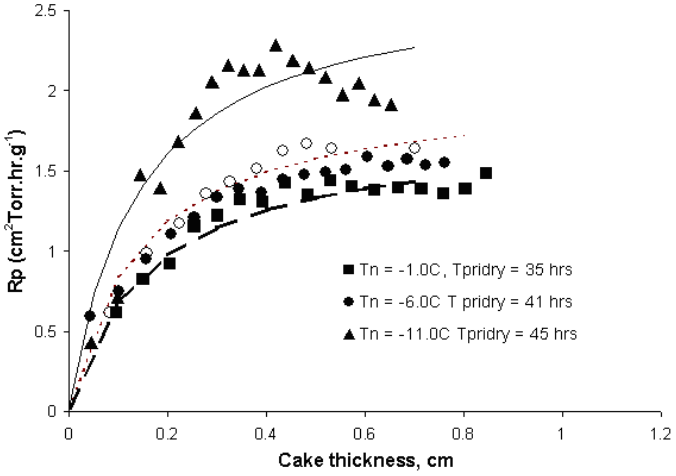

Figure 2. Resistance, $\hat{R}_{ps}$, ($\hat{R}_{ps} = \hat{R}_p + \hat{R}_s$) as a function of dry layer thickness obtained using the improved ice fog technique (Method II) for 5% wt/vol sucrose at 3 different nucleation temperatures. Replicates are shown as open symbols. $\langle \hat{R}_p \rangle$ values in cm^2 · Torr · hr · g^{-1} during primary drying are 1.35 (-1°C), 1.61 (-6°C), and 2.01 (-11°C).cm^2 · Torr · hr · g^{-1}.

of –25°C and a chamber pressure of 100 mTorr. Product resistance data for samples corresponding to each of the 3 nucleation temperatures are shown in Figure 1. Note that no systematic difference in product resistance arising from the differences in nucleation temperature are obvious although primary drying times increased by 10% for an 8°C increase in the degree of supercooling. However, the impact of variation in nucleation temperature in this experiment is likely reduced by annealing during the freezing procedure. The long times required for complete nucleation (~30 minutes), with the sample far above the Tg′ (–34°C),[3] provide favorable conditions for annealing and Ostwald ripening. As a result of Ostwald ripening the heterogeneity in product resistance arising due to differences in nucleation temperature is minimized and product resistance is decreased significantly in the case of samples with higher degrees of supercooling.[3] Hence, product resistance data do not differ greatly due to differences in nucleation temperature. In addition, the flattening of the resistance curve with thickness (Figure 1) suggests the onset of "microcollapse" (the maximum product temperature during primary drying was –32°C) in the cake and a further reduction in product resistance, a phenomenon commonly observed with low collapse temperature materials.[9] This effect would also "level" the effects of the initial variation in pore size.

Improved Ice Fog Technique: Method 2

The observations made during our previous study with sucrose suggest a need to decrease the time required for nucleation in order to minimize the effects of Ostwald ripening. The temperature of the nitrogen entering the chamber was reduced to <–50°C by shortening the length (< 1 ft) of tubes leading from the dewar of liquid nitrogen to the chamber. Shorter tubing minimized heat exchange with ambient. Also, the tube inside the chamber was constructed in the form of a circular ring (~8-inch diameter) and attached to the shelf above the vials. Several holes (~0.18-inch diameter, 2 inches apart) were punched along the circumference of the tube, thus enabling the cold gas to be distributed more evenly throughout the chamber. The pressure of nitrogen was maintained at 10 psi. Visual observations indicated that the "ice fog" was denser throughout the chamber compared with our earlier studies using method 1. These improvements resulted in much faster nucleation times, and nucleation of all samples on the shelf was achieved in less than 5 minutes. Figure 2 shows product resistance data for sucrose obtained as a function of cake thickness at 3 different nucleation temperatures using the improved ice fog technique. Clearly, there is an impact of degree of supercooling on product resistance as well as the anticipated effect on primary drying time. Primary drying times are longer for lower nucleation temperature, and differences in $\langle \hat{R}_p \rangle$ are consistent with drying times. Lines represent smoothed $\hat{R}_p$ data from values of A_1 and A_2 (Equation 6). Samples nucleated at –11°C resulted in much higher product resistances with the primary drying time nearly 30% higher when compared with samples nucleated at –1°C. The maximum product temperature was –32°C during primary drying. Here, the product temperature is close to the glass transition temperature, which suggests that "microcollapse" of structure does take place. The flattening of the resistance curve in Figure 2 is an indication that "microcollapse" may have impacted the data.

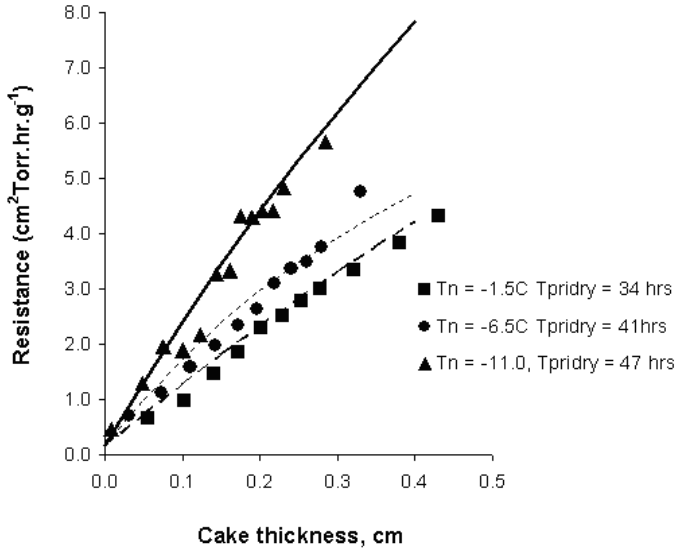

Figure 3. Resistance, $\hat{R}_{ps}$, ($\hat{R}_{ps} = \hat{R}_p + \hat{R}_s$) as a function of dry layer thickness obtained for 5% wt/vol HES at 3 different nucleation temperatures. $\langle \hat{R}_p \rangle$ values in cm² · Torr · hr · g⁻¹ during primary drying are 4.66 (-1.5°C), 5.00 (-6.5°C), and 7.50 (-9.5°C).

The improved ice fog technique was also used to achieve different degrees of supercooling for the other excipients studied (ie, HES, dextran, and mannitol). Behavior for each excipient is described as follows:

HES

The collapse temperature of a 5% wt/vol HES solution was determined to be approximately –11°C from freeze-drying microscopy experiments (data not shown). Primary drying was conducted at a shelf temperature of –20°C and a chamber pressure of 100 mTorr, the maximum product temperature during primary drying being –33°C. Thus, primary drying was performed well below the collapse temperature. Product resistance data obtained for samples of HES nucleated at 3 different temperatures (–1°C, –7°C, and –11°C) are shown in Figure 3. Similar to data obtained for sucrose, a higher degree of supercooling resulted in much higher product resistances and correspondingly longer primary drying times. However, product resistance profiles as a function of cake thickness were qualitatively different from that obtained for sucrose in that the resistance curve did not flatten off with increasing dry layer thickness, consistent with the expectation that HES would not undergo microcollapse in a process where the product temperature is far below the collapse temperature.

Dextran

The collapse temperature of a 5% wt/vol dextran solution was determined to be approximately –13.5°C from freeze-drying microscopy experiments (data not shown). Primary drying shelf temperatures and chamber pressures were maintained at 0°C and 120 mTorr respectively. The maximum product temperature during primary drying was –26°C. Product resistance data obtained as a function of cake thickness at 3 different nucleation temperatures (–1°C, –7°C, and –11°C) during primary drying are shown in Figure 4. Similar to data obtained for the other 2 excipients, product resistance increases as ice nucleation temperature decreases.

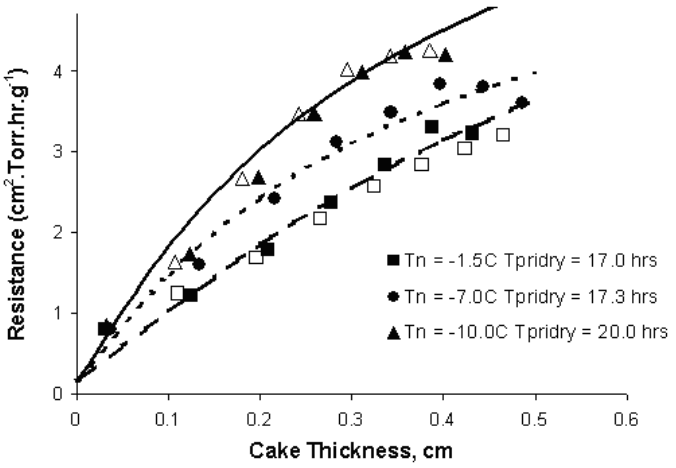

Figure 4. Resistance, $\hat{R}_{ps}$, ($\hat{R}_{ps} = \hat{R}_p + \hat{R}_s$) as a function of dry layer thickness obtained using the improved ice fog technique (Method II) for 5% wt/vol dextran at 3 different nucleation temperatures. Replicates are shown as open symbols $\langle \hat{R}_p \rangle$ values in cm² · Torr · hr · g⁻¹ during primary drying are 3.64 (-1.5°C), 3.81 (-7°C), and 4.41 (-10°C).

Mannitol

Freeze drying of mannitol was performed at a shelf temperature of +5°C and a chamber pressure of 100 mTorr. Mannitol provides an example of a crystalline product. Since the freezing procedure used enables crystallization of mannitol during freezing itself, vial breakage, a feature commonly associated with the crystallization of mannitol during primary drying, is not an issue.[11] Similar to our observations with the amorphous excipients, product resistance and ice nucleation temperature are correlated with higher resistance corresponding to lower nucleation temperatures (Figure 5).

Thus, it appears that both amorphous and crystalline products show the same qualitative correlation between ice nucleation temperature and resistance.

Intervial heterogeneity in nucleation temperature commonly observed in freeze-drying experiments should therefore be either avoided or compensated for during process development. While the ice fog technique was successfully implemented for temperature-controlled nucleation, a significant limitation of laboratory scale freeze drying was the inability to achieve higher degrees of supercooling. Nonetheless, with

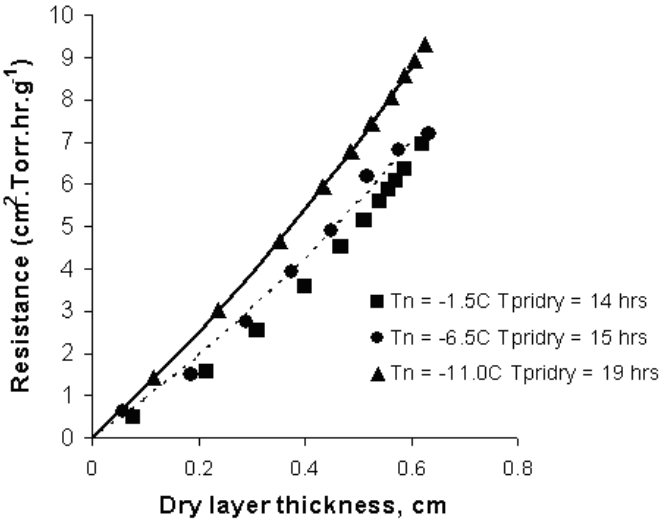

Figure 5. Resistance, $\hat{R}_{ps}$, ($\hat{R}_{ps} = \hat{R}_p + \hat{R}_s$) as a function of dry layer thickness obtained using the improved ice fog technique for 5% wt/vol mannitol at 3 different nucleation temperatures. $\langle \hat{R}_p \rangle$ values in cm² · Torr · hr · g⁻¹ during primary drying are 6.24 (-1.5°C), 7.00 (-6.5°C), and 7.73 (-11°C).

a suitable correlation, the data obtained should be capable of reliable extrapolation to the higher degrees of supercooling commonly observed in manufacturing operations.

Specific Surface Area Measurements

All of the samples freeze dried using the protocols described above were analyzed for specific surface area (m^2/g). The specific surface area of a material is a reflection of the pore size, which in turn is a reflection of the size and morphology of the ice crystals. If we imagine the porous solid is a slab composed of n cylindrical pores of radius r and length L, the specific surface area of the pores may be expressed as

$$SSA = \frac{n \cdot 2\pi rL}{\rho_s V_s} \qquad (2)$$

where ρ_s is the density of the solid and V_s is the solid volume. Note that this model is the "capillary tube" model for a porous system and is not likely to be highly accurate. However, we only seek a basic understanding of how specific surface area is likely to be related to resistance of the dry product layer to mass transfer, $\hat{R}_p$. Expressing V_s in terms of the total volume ($\pi R^2 L$) and the void volume fraction, ε ($\varepsilon = \frac{V_{void}}{V_{total}} = \frac{nr^2}{R^2}$), we have

$$SSA = \frac{n \cdot 2\pi rL}{\rho_s(1-\varepsilon)\pi R^2 L} = \frac{2(\frac{nr^2}{R^2})}{r\rho_s(1-\varepsilon)} \qquad (3)$$

Table 1. BET Specific Surface Area (SSA) Measurement of Freeze-dried Cakes Nucleated at Different Nucleation Temperatures, T_n. Surface Areas Are Represented as Mean ± Standard Deviation for 3 Measurements

Excipient	T_n (°C)	SSA (m^2/g)
Sucrose	-1.0	0.32 ± 0.03
	-6.0	0.42 ± 0.03
	-11.0	0.61 ± 0.03
Dextran	-1.5	0.37 ±0.14
	-7.0	0.57 ± 0.06
	-10.0	0.71 ± 0.03
HES	-1.5	0.85 ± 0.02
	-6.5	0.87 ±0.04
	-9.5	1.08 ± 0.05
Mannitol	-1.5	3.64 ± 0.24
	-6.5	3.94 ± 0.45
	-10.0	4.45 ± 0.43

where R is the total radius and "1-ε" is the solute concentration in volume fraction units. Therefore,

$$SSA = \frac{2\varepsilon}{\rho_s(1-\varepsilon)} \cdot \frac{1}{r} \qquad (4)$$

Hence, the smaller the radius of the pores, larger is the value of specific surface area, SSA.

Since at constant solids content, the SSA depends only on pore size (in this simple model) and since nucleation temperature is the major factor in determining pore size, one would expect SSA and degree of supercooling to be well correlated. Table 1 shows BET specific surface areas of samples freeze dried after nucleating at different temperatures. Average specific surface areas of 3 samples picked at random from the array of vials are shown. Values of SSA are higher for mannitol, presumably because of its crystalline nature. Also, absolute standard deviations in specific surface area are higher in the case of mannitol. A trend in specific surface area with degree of supercooling is observed for all of the materials studied. That is, we observe an increase in product specific surface area with an increase in the degree of supercooling. For mannitol, the trend is the same as with the other solutes, but the differences in specific surface area are not statistically significant. In the context of this study, it is important that the nucleation temperature be relatively constant for all of the samples in a given freeze-dried batch. The low standard deviations in SSA are a reflection of the intervial homogeneity in ice nucleation temperature, which was achieved by use of the improved ice fog technique. For comparison, we note that we had obtained a value of 0.88 ± 0.20 from experiments with sucrose where freezing was done without the ice fog procedure, nearly an order of magnitude larger standard deviation than that shown in Table 1 for the ice fog technique. The trend in specific surface area with degree of supercooling (Table 1) suggests that one may estimate specif-

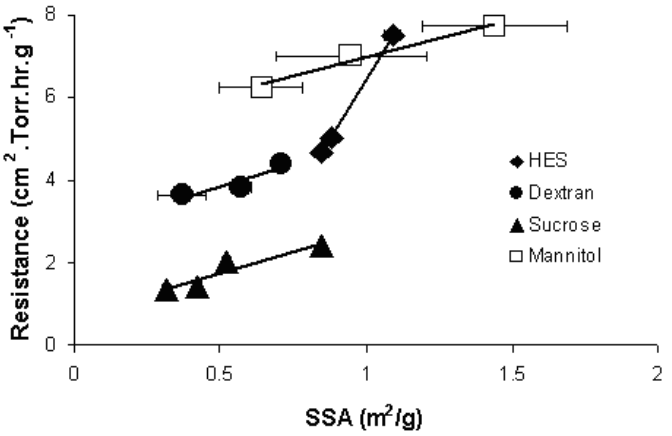

Figure 6. Average resistance, $\langle \hat{R}_p \rangle$, as a function of specific surface area (SSA) for different excipients. Average product resistance values are determined over a cake thickness of 1 cm. Lines represent linear fit to the data. The slopes are 2.06 (sucrose), 2.16 (dextran), 1.82 (mannitol), and 11.86 (HES). Error bars represent the standard error in SSA values.

ic surface area of samples freeze dried in manufacturing scale lyophilizers where solutions typically experience ~20°C supercooling by linear extrapolation.

SSA and Product Resistance

Here we attempt to correlate the specific surface area with the resistance of the product. Assuming that the porous cake of thickness, l, and porosity, ε, created during freeze drying is a collection of capillary tubes of radius, r, the dry layer resistance may be written as:

$$\hat{R}_p = \sqrt{\frac{\pi RT}{2M}} \cdot \frac{3}{4} \cdot \frac{\tau^2}{\varepsilon} \cdot \left(\frac{l}{r}\right) \qquad (5)$$

where the tortuosity, τ, is the ratio of the total channel length to the thickness of the porous system. Here, RT is the product of the gas constant and absolute temperature, and M is the molecular weight of water. The void volume fraction is ε, the cake thickness is l, and the pore radius is r. τ is frequently taken to be ≈1.5.[12] Thus, at least from this simple model, we expect the dry layer resistance to be determined largely by the pore radius and therefore to correlate directly with the SSA (see Equation 4) and also to then correlate with the degree of supercooling. In real systems, the dry layer resistance is not necessarily directly proportional to cake thickness, as implied by Equation 5, so we seek a "one parameter" measure of the entire resistance vs thickness curve. For this purpose we choose the average resistance over a thickness range of 1 cm, denoted $\langle \hat{R}_p \rangle$. While the maximum dry layer thickness may not be 1 cm in the application of interest, this parameter still serves as a single parameter measure of resistance for correlation purposes. In order to express the average product resistance as a function of cake thickness, values of the parameters A_1 and A_2 were determined by fitting the equation describing product resistance behavior, $\hat{R}_p$, as a function of cake thickness, l to the data.[13]

$$\hat{R}_p = R_p(0) + \frac{A_1 \cdot l}{1 + A_2 \cdot l} \qquad (6)$$

Figure 6 shows plots of average product resistance as a function of specific surface area for each of the materials freeze dried under different conditions. A value of 3.0 was subtracted from the specific surface area of mannitol so that mannitol data could be shown on the same plot. A linear fit to the data suggests that with the exception of HES, values of the slopes are very similar. The linear plot of dextran, sucrose, and mannitol suggests that the resistance increases by ~2 ($cm^2 \cdot Torr \cdot hr \cdot g^{-1}$) for an increase in SSA of 1 m^2/g. It is interesting that combination of Equations 4 and 5 gives close to the same numerical result for a "typical" system (1.3 $cm^2 \cdot Torr \cdot hr \cdot g^{-1}$). The linear relationship between $\hat{R}_p$ and SSA with the slope determined by experiment for the product of interest should be useful for the estimation of product resistance in a manufacturing process and provide a rational basis for scale-up.

As an example of how one might use SSA data to scale up a freeze-drying process, we construct a hypothetical but realistic case. Consider a product that is being freeze dried in the laboratory with a fill depth of 0.75 cm that we wish to freeze dry with the same thermal history in manufacturing as we find in the laboratory (In the laboratory we use a chamber pressure of 60 mTorr and a shelf temperature of -30°C during primary drying to produce a product temperature in primary drying of -37.1°C and primary drying time of 40.7 hours). We have determined in the laboratory that the average nucleation temperature is –10°C, the mean product resistance, $\langle \hat{R}_p \rangle$, is 4.3 $cm^2 \cdot Torr \cdot hr \cdot g^{-1}$, and the SSA is 0.71 m^2/g. We also find that the increase in mean resistance per 1 m^2/g increase in SSA is 2.17 m^2/g. We further find that the measured SSA in a non-optimized clinical trial run (ie, with ice nucleation expected to be the same as in manufacturing) is 1.1 m^2/g. Thus, we project that the mean resistance for material produced in manufacturing would be

$$\langle \hat{R}_p \rangle = 4.3 + 2.17(1.1–0.71) = 5.15 \ cm^2 \cdot Torr \cdot hr \cdot g^{-1}.$$

Impact of Product Resistance Differences on Product Temperature and Primary Drying Time

Steady-state heat and mass transfer equations were used to predict the impact of differences in product resistance on

the product temperature during primary drying and consequently, on the primary drying time. The rate of sublimation in steady state is given by Equation 1, and the rate of heat transfer is given in terms of the vial heat transfer coefficient, K_v, and the shelf temperature, T_s, by

$$\frac{dQ}{dt} = A_v \cdot K_v \cdot (T_s - T - \Delta T) \qquad (7)$$

where T is the temperature of the subliming ice, and ΔT is the temperature difference across the frozen layer. Assume, for this example, that the vial heat transfer coefficient is 3.7 10^{-4} $cals^{-1}cm^{-2}K^{-1}$. In the example given here, ΔT may be assumed constant at 0.1°C. Since heat and mass transfer are coupled by, $dQ/dt = \Delta H_s\ (dm/dt)$, with ΔH_s being the heat of sublimation, we may write,

$$P_0 - P_c - \frac{A_v}{A_p}\ (10^4 K_v)\cdot(T_s - T - \Delta T)\cdot\ \frac{\hat{R}_{ps}}{1833} = 0 \qquad (8)$$

where $\hat{R}_{ps}$ denotes the sum of the area normalized product and stopper resistances, and P_0 is the vapor pressure of ice,

$$\ln P_0 = \frac{6144.96}{T} + 24.0185 \qquad (9)$$

A_v is the cross-sectional area of the vial calculated from the outer diameter, and the number "1833" comes from units conversion and the heat of sublimation of ice. Given fixed values of shelf temperature, chamber pressure, and resistance, Equations 8 and 9 may be solved for temperature and then Equation 1 may be used to evaluate the sublimation rate. If we identify the resistance and temperature in Equations 8 and 9 as mean values, we may input mean value resistance and solve for mean temperature and mean sublimation rate, thereby allowing the primary drying time to be evaluated from the mean sublimation rate and fill volume of water.

In our example, input of 4.3 $cm^2 \cdot Torr \cdot hr \cdot g^{-1}$ for resistance gives a mean product temperature of –37.1°C and a mean primary drying time of 40.7 hours. Input of 5.15 $cm^2 \cdot Torr \cdot hr \cdot g^{-1}$ for the mean resistance, corresponding to our estimate for product produced in manufacturing, gives –36.6°C for the mean product temperature and 43.9 hours for the mean primary drying time. Since the projected temperature in manufacturing is only slightly higher than found in the laboratory, one may simply ignore the temperature difference as negligible. However, the drying time is projected to be 3 hours longer, which means the manufacturing cycle should include a holding time or "soak time" which is 3 hours longer than used in the laboratory. Alternately, one might argue that it is necessary to run the same product temperature in manufacturing as in the laboratory. Thus, one may lower the shelf temperature slightly to produce equivalent product temperatures. Running the shelf temperature at –31°C produces a mean product temperature of –37.0°C, almost identical to the laboratory process. Here, the primary drying time is 47.9 hours, and the manufacturing cycle would need to extend primary drying 7.2 hours beyond the laboratory cycle, a significant extension!

Conclusion

The impact of the degree of supercooling on the product resistance cannot be ignored during scale up. Differences in the degree of supercooling between laboratory and manufacturing may lead to significant variations in drying time and to product collapse. The present study emphasizes the importance of this scale-up issue and suggests that a correlation between the product resistance and the specific surface area will help in quantitative prediction of the impact of freezing variations during scale up.

The ice fog technique has been successfully implemented as a means of controlling the nucleation temperature within vials of the same batch. Although this technique was not fully optimized and does require more work in order to be implemented in commercial freeze-drying operations, it is a promising technique for temperature-controlled nucleation.

Acknowledgments

The authors wish to thank Xiaolin (Charlie) Tang for his help with MTM and with analyzing MTM data. Jean-Philippe Obert is acknowledged for his suggestions with improving the ice fog technique. This project was funded by the National Science Foundation–Center for Pharmaceutical Processing Research (NSF-CPPR). Roee Ramot received financial support from a summer fellowship funded by Boehringer-Ingelheim Pharmaceuticals Inc.

References

1. Pikal MJ, Rambhatla S, Ramot R. The impact of the freezing stage in lyophilization: effects of the ice nucleation temperature on process design and product quality. *American Pharmaceutical Review*. 2002;5:48-52.

2. Pikal MJ. Freeze drying. In: Swarbrick J, Boylan J, eds. *Encyclopedia of Pharmaceutical Technology*. New York: Marcel Dekker; 2001.

3. Searles JA, Carpenter JF, Randolph TW. Annealing to optimize the primary drying rate, reduce freezing-induced drying rate heterogeneity, and determine T-g′ in pharmaceutical lyophilization. *J Pharm Sci*. 2001;90:872-887.

4. Searles JA, Carpenter JF, Randolph TW. The ice nucleation temperature determines the primary drying rate of lyophilization for samples frozen on a temperature-controlled shelf. *J Pharm Sci*. 2001;90:860-871.

5. Kochs M, Korber C, Nunner B, Heschel I. The influence of the freezing process on vapor transport during sublimation in vacuum-freeze-drying. *Int J of Heat and Mass Transfer.* 1991; 34:2395-2408.

6. Roy ML, Pikal MJ. Process control in freeze drying: determination of the end point of sublimation drying by an electronic moisture sensor. *J Parenter Sci Technol*. 1989;43:60-66.

7. Rowe TD. A technique for the nucleation of ice. Paper presented at: International Symposium on Biological Product Freeze-Drying and Formulation; October 26, 1990; Geneva, Switzerland.

8. Rambhatla S, Pikal MJ. Heat and mass transfer scale up issues during freeze-drying. Part I. Atypical radiation and the edge-vial effect. *AAPS PharmSciTech*. 2003;4:E14.

9. Milton N, Pikal MJ, Roy ML, Nail SL. Evaluation of manometric temperature measurement as a method of monitoring product temperature during lyophilization. *PDA J Pharm Sci Technol*. 1997;51:7-16.

10. Pikal MJ, Roy ML, Shah S. Mass and heat transfer in vial freeze-drying of pharmaceuticals: role of the vial. *J Pharm Sci*. 1984;73:1224-1237.

11. Adenyika WN, Thomas D. Vial breakage by frozen mannitol solutions: correlation with thermal characteristics and effect of stereoisomerism, additives, and vial configuration. *J Parenter Sci Technol*. 1991;45:94-100.

12. Pikal MJ. Heat and mass transfer in low pressure gases: applications to freeze drying. In: Amidon G, Lee P, Topp L, eds. *Transport Process in Pharmaceutical Systems*. New York: Marcel Dekker; 1999.

13. Pikal MJ. Use of laboratory data in freeze drying process design: heat and mass transfer coefficients and the computer simulation of freeze drying. *J Parenter Sci Technol*. 1985;39:115-139.